

# PHANTOM STUDY USING A FIRST GENERATION GAMMA TOMOGRAPHY SYSTEM

**Pablo A. S. Vasquez<sup>1</sup>, Carlos H. de Mesquita<sup>1</sup> and Margarida M. Hamada<sup>1</sup>**

<sup>1</sup> Instituto de Pesquisas Energéticas e Nucleares (IPEN / CNEN - SP)  
Av. Professor Lineu Prestes 2242  
05508-000 São Paulo, SP  
mmhamada@ipen.br  
pavsalva@usp.br

## ABSTRACT

A first generation parallel beam computed tomography (CT) scanner system was used in this study. Several experiments were made using a polypropylene cylindrical IAEA phantom with 400 mm diameter and 0,91 g/cm<sup>3</sup> density. The CT scanner consists of a NaI(Tl) detector with a 5.08 cm diameter and a sealed <sup>60</sup>Co radioactive source located opposite to the center of the detector. The detector and the source are mounted on fix support and the phantom can be rotated and dislocated by two stepping motors controlled by a microprocessor. The detector side collimator provides 5mm width collimated  $\gamma$  - rays to the detector. In each movement, the phantom rotates by 6°. To obtain statistical significant results and to reduce the effect of the position, the CT scans were obtained by scanning 360° using a total scanning time of about 4 hours and collecting numerous beam path attenuations (approximately 6400). The source activity was calculated using the JANU simulation software (325  $\mu$ Ci). The results are showed as sinograms surface plots and reconstructed tomograms plots for different conditions: counting time, internal density and electronic discrimination detector. The software used the filtered back-projection algorithm to perform the inverse Radon transform for parallel projection data. Linear interpolation and the cropped Ram-Lak are used in this software. Additional plots show 3D- volumetric reconstructions using different 2D slices data under the same conditions.

## 1. INTRODUCTION

Since their discovery and first use for the examination of materials, ionizing radiation have been extensively used, chiefly in the last three decades, to investigate the internal structure of a great diversity of samples. In spite of its incontestable advantages in revealing the internal structure of the examined objects, the classical radiographic method has two major disadvantages. The first one consists of the fact that all details of the investigated sample are projected, irrespective of their position, onto the same plane [1].

Consequently, a considerable amount of information concerning the relative position within the sample volume of various details is lost. The second one is related to the nonlinear response of the radiosensitive emulsion, i.e., the optical density vs. the logarithm of the absorbed dose of radiation is represented following a sigmoidal (S- shaped) curve instead of a linear one. Consequently, between the optical density and the linear attenuation coefficients there is a non-linear dependency. This circumstance is a source of systematic errors for any quantitative determination of sample density. These disadvantages have been overcome by a new method of investigation, developed since 1973, i.e., computer tomography (CT).

This method represents one of the most promising techniques of investigation based upon the attenuation of the nuclear radiation (X-and gamma-ray, neutrons). In contrast to classical X-ray tomography, CT generates the images that are not influenced by the matter outside the

investigated section and therefore presents an increased spatial resolution. Initially developed as a medical imaging technique (Oldendorf, 1961; Cormack, 1963; Hounsfield, 1972); CAT proved to possess a remarkable ability in revealing with precision and accuracy the spatial distribution of details which compose the inner structure of the considered objects. For that reason, CT has been rapidly applied to other domains of the sciences.

## 2. PRINCIPLE

Tomography with ionizing radiation is based on obtaining projections of the density distribution inside the object area by measuring the attenuation of the radiation emitted by a source placed on one side of the object, and measured by one or more detectors situated at the opposite side. Classical arrangements consist of a fan-beam source and a row or an arc of detectors. Thus, one-dimensional projections of the two-dimensional density distribution, inside the measuring cross section, are obtained at once. A set of independent projections for different angles is recorded by rotating source and detector array around the object. The distribution inside the measuring cross section is recovered using tomographic image reconstruction methods. Instead of rotating the tomograph around the object, it is also possible to rotate the object itself. There are also reports about tomography systems using a conical beam and a two dimensional detector array [1]. In this case a three dimensional image reconstruction is carried out.

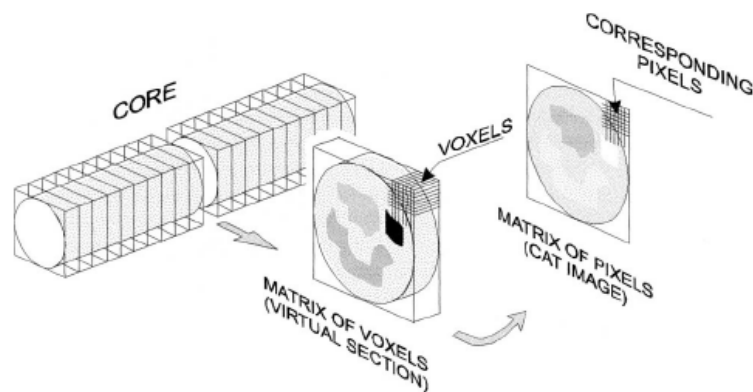


**Figure 1. Schematic representation of the relation between the investigated object and its CT image. As result of the reconstruction algorithm, this section is decomposed into volume elements (voxels). Each voxel is characterized by an average value of the linear attenuation coefficient.**

As a method of investigation based on the attenuation of X or gamma-ray, CT maps the distribution of the linear attenuation coefficients of the sample over an entire transverse section (Fig. 1). X- or gamma-ray interacts with the matter by means of four effects, i.e., Raleigh (coherent scattering), photoelectric effect, Compton Effect and pair generation (Siegbahn, 1967). All these interactions depend, in a specific way, upon photon energy as well as the atomic number of the absorber. Therefore, at its passage through the matter, a thin, well collimated beam of X- or gamma-ray is attenuated following Beer's law [2].

For inhomogeneous samples, the attenuation coefficient has different values for different points of the investigated object. Therefore, by determining the numerical values of this coefficient for any point of the object, a significant amount of information concerning both the chemical composition and the density of the sample could be obtained. When measuring the attenuation of a thin beam of radiation, for a constant distance between source and detector permits one to determine the projection of the linear attenuation coefficient on specifically direction [2].

By sending a great number of coplanar radiation beams through the object, an equal number of projections could be measured simultaneously. As all beams are coplanar, the corresponding projections will determine a section through object. By using an appropriate reconstruction algorithm (Herman, 1980; Herman and Natterer, 1981; Natterer, 1986), the numerical values of all projections allow one to determine the two-dimension distribution function of the linear attenuation coefficient onto the section. Because the number of projections is finite (about 105–106), it follows that the number of values of this coefficient onto the investigated section will be also finite. In this way, the investigated section will be decomposed in a number of volume units, having a prismatic shape, called voxels (an acronym for volume element).

Consequently, each voxel, whose dimensions are roughly equal to the X- or gamma-ray beam diameter, is characterized by a single value of the linear attenuation coefficient. Further, to each voxel a pixel of image can be attributed to shades of gray and are proportional to the corresponding numerical value of the attenuation coefficient. Finally, this results a two-dimension map representing the distribution of the linear attenuation coefficient over the entire section, whose spatial resolution is equal to the voxel size. This picture, which represents the reconstruction of the distribution function of the  $\mu$  coefficient by means of its projection, is the final CT image. By assembling together a great number of consecutive and parallel CT digital images, it results in a complete three-dimensions matrix of data containing the distribution of the attention coefficient over the entire object. In order to reveal as many as possible details, these data can be subsequently used to obtain new CT images following any desired section [2,3,4].

### 3. EXPERIMENTAL SET-UP

The experimental setup, schematically shown in Fig.2 as developed to study the IAEA phantom (diameter 400 mm).

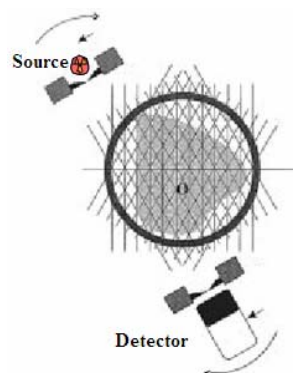


**Figure 2. Schematic diagram of the computed tomograph.**

A first generation parallel beam computed tomography (CT) scanner system [3] was used in this study. The CT scanner consists of a NaI(Tl) detector with a 5.08 cm diameter and an encapsulated  $^{60}\text{Co}$  radioactive source located opposite to the center of the detector. The detector and the source were mounted on fix support and the phantom can be rotated and dislocated by two stepping motors controlled through a microprocessor. The detector side collimator provided 5mm width collimated  $\gamma$  - rays to the detector. In each movement, the phantom was rotated by  $6^\circ$ .

To obtain statistical significant results and to reduce the effect of the position, the CT scans were obtained by scanning  $360^\circ$  using a total scanning time about 4 hours and collecting numerous beam path attenuations (approximately 6400).

The source activity was calculated using JANU simulation software. For this phantom the minimal effective required activity was  $325 \mu\text{Ci}$  with a confidence level of 95 % and 1% relative error for 10s counting time.

The software uses the filtered back-projection algorithm to perform the inverse Radon transform for parallel projection data. The filter is designed directly in the frequency domain and then multiplied by the FFT of the projections. The projections are zero-padded to a power of 2 before filtering to prevent spatial domain aliasing and to speed up the FFT [2]. The computational program reconstructs the image from projection data in the two-dimensional array using a matrix where the columns are parallel beam projection data for different angles (in degrees) at which the projections were taken. The software assumes that the center of rotation is the center point of the projections. Linear interpolation and the cropped Ram-Lak are used in this software [2,3].

#### 4. RESULTS AND DISCUSSION

The results are showed using reconstructed tomograms including the root mean square errors (RMSE) respect N (total pixels number) and  $\mu$  (attenuation coefficient) and the specific conditions. In all cases were used lead collimators for the source and the detector. Fig. 3 represents the projection values in a sinogram and a surface plots for the first study case.

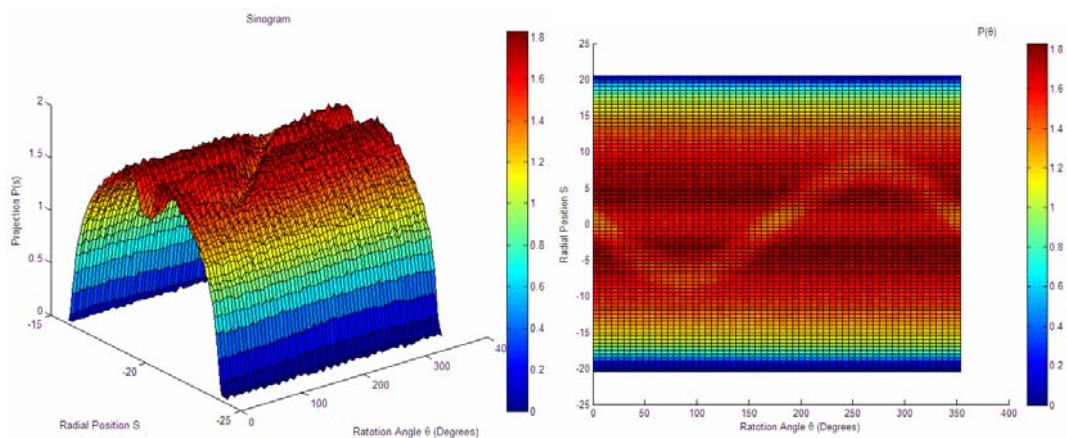


**Figure 3. Sinogram and surface projection plots.**

Experimental conditions to improve the reconstructed images as counting time, internal density and electronic discrimination detector were tested in different study cases showed the attenuation coefficient  $\text{cm}^{-1}$  ( $\mu$ ) vs. the position X(cm) and Y(cm) in the Fig. 4. The first case (1) shows the results working with a collimator width of 5 mm and a counting time of 15 s,  $\text{RMSE}(N) = 1.7045 \times 10^{-4}$ ;  $\text{RMSE}(\mu) = 1.2864 \times 10^{-4}$ . The second (2) case represents a collimator width of 5 mm, a counting time of 15 s with the central phantom hole filled with oil ( $0.9 \text{ g/cm}^3$ );  $\text{RMSE}(N) = 1.2864 \times 10^{-4}$ ;  $\text{RMSE}(\mu) = 2.2710 \times 10^{-1}$ . The third (3) case represents a collimator width of 5 mm, counting time of 20 s with both of phantom holes filled with lead plugs;  $\text{RMSE}(N) = 6.3555 \times 10^{-4}$ ;  $\text{RMSE}(\mu) = 4.4298 \times 10^{-1}$ . The fourth (4) case represents a collimator width of 5 mm, a counting time of 20 s with the external phantom hole filled with a lead plug;  $\text{RMSE}(N) = 3.7868 \times 10^{-4}$ ;  $\text{RMSE}(\mu) = 3.6955 \times 10^{-1}$ . The fifth (5) shows the results working with the same conditions of case 4 but with a counting time of 15s;  $\text{RMSE}(N) = 3.6180 \times 10^{-4}$ ;  $\text{RMSE}(\mu) = 3.9372 \times 10^{-1}$ . The sixth (6) case represents the same conditions of the case 4 but with a counting time of 5s;  $\text{RMSE}(N) = 3.7587 \times 10^{-4}$ ;  $\text{RMSE}(\mu) = 3.6584 \times 10^{-1}$ . The seventh (7) case represents the same condition of the case 4 but working into the photopick discrimination region,  $\text{RMSE}(N) = 4.6180 \times 10^{-4}$ ,  $\text{RMSE}(\mu) = 4.3600 \times 10^{-1}$ . The eighth (8) plot represents the surface reconstructed tomogram for case 1.

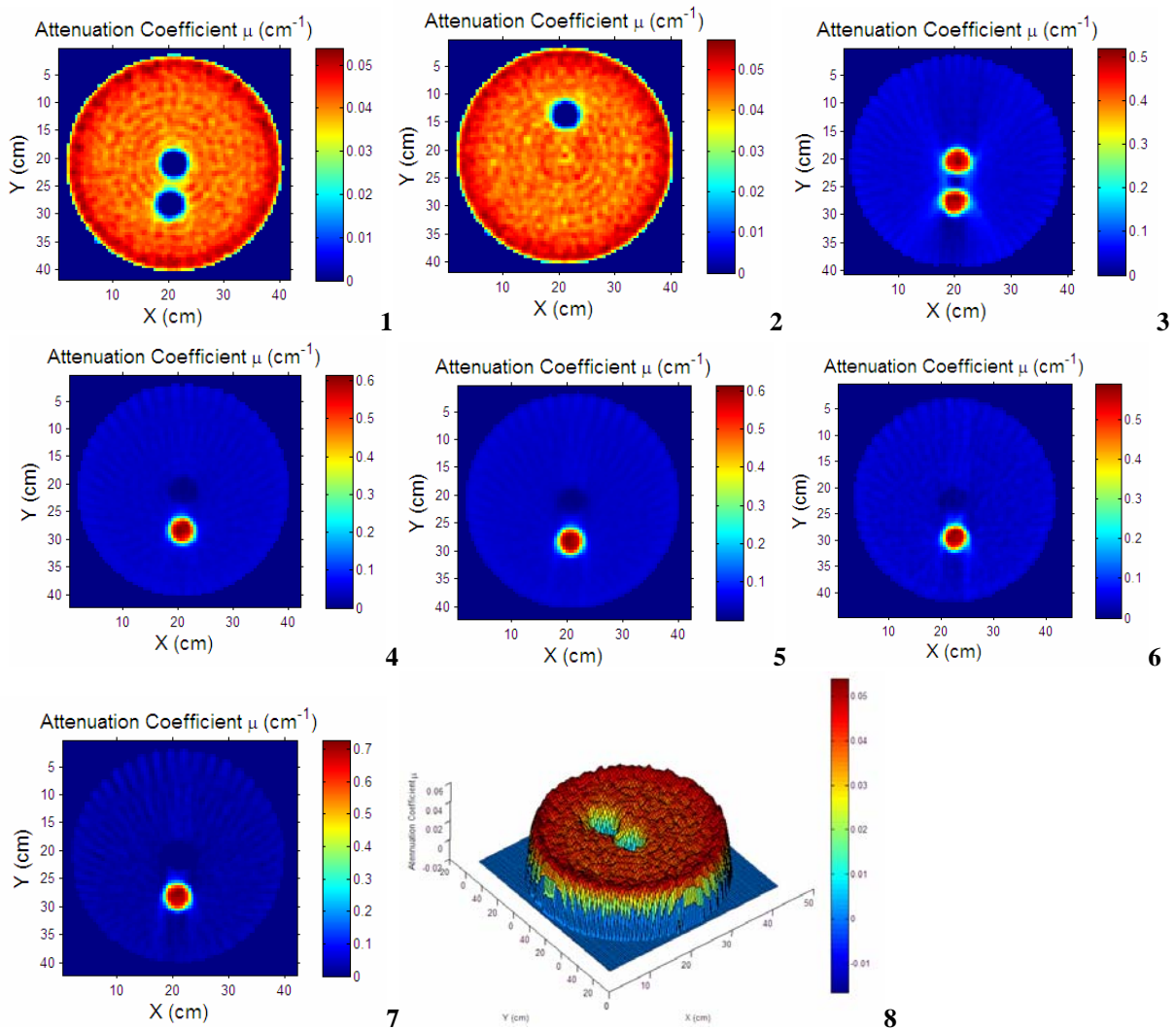


**Figure 4. Reconstructed tomographic images using different parameters.**

The next plots (Fig. 5) show 3D- volumetric reconstructions using different 2D slices data under the same conditions. The images were reconstructed with the box – Gaussian convolution kernel smoothing voxel method. Fig shows the 3D plots for the cases 1, 2, 3 and 4 using different views [5].

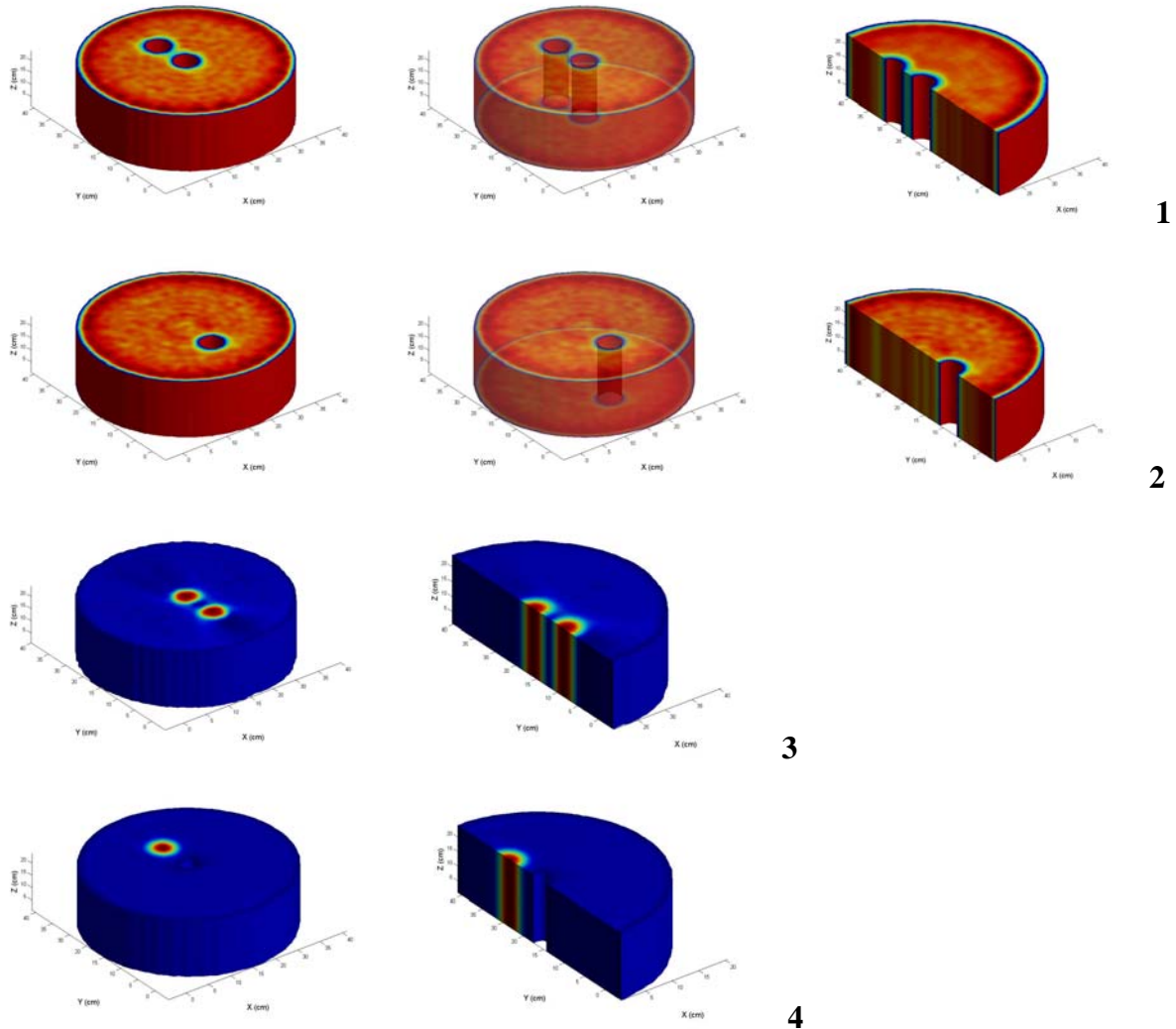


**Figure 5. 3D-Reconstructed plots: normal, transparent and cross section views for 1, 2, 3 and 4 cases.**

### 3. CONCLUSIONS

A first generation gamma tomograph developed for this work showed high performance to study static objects. To obtain acceptable image results is not necessary long counting times and, depending on the phantom density, is possible to work without restriction in the detector electronic discrimination. The system is able to distinguish materials with very different densities easily, but this depends on of the sealed source used. The algorithms used to reconstruct the images 2D and 3D were useful and of quick application.

## ACKNOWLEDGMENTS

The authors would like to thank to Conselho Nacional de Desenvolvimento Científico e Tecnológico (CNPq) and to Atomic Energy Agency International (IAEA) for the financial support.

## REFERENCES

1. Chaouki, F.; Larachi, ; Dudukovic, M.P., Noninvasive Tomographic and Velocimetric Monitoring of Multiphase Flows, *Ind. Eng. Chem. Res.*, 1997, 36, pp. 4476-4503.
2. Kak, A. C., and M. Slaney, Principles of Computerized Tomographic Imaging, New York, NY, IEEE Press, 1988.
3. Bracewell, Ronald N., Two-Dimensional Imaging, Englewood Cliffs, NJ, Prentice Hall, 1995, pp. 505-537.
4. Lim, Jae S., Two-Dimensional Signal and Image Processing, Englewood Cliffs, NJ, Prentice Hall, 1990, pp. 42-45.
5. Gonzalez, R.C.; Woods, R.E., Digital Image Processing, Pearson Prentice-Hall, 2004.
6. <http://physics.nist.gov>